

Modeling of low temperature adsorption of hydrogen in carbon nanopores

Justyna Rogacka¹ · Lucyna Firlej^{2,3} · Bogdan Kuchta^{1,3,4} 

Received: 14 October 2016 / Accepted: 16 December 2016 / Published online: 3 January 2017
© Springer-Verlag Berlin Heidelberg 2016

Abstract We simulated the low temperature ($T = 77$ K) hydrogen adsorption in carbon slit-shaped nanopores using consecutively united atom (UA) and all atom (AA) representation of hydrogen molecule. We showed that both approximations give comparable estimation of the amount stored, for the wide range of pore width (0.6–2.5 nm). We also showed that at very high pressure ($P = 400$ bar, corresponding to the fugacity $f = 800$ bar) the density of the adsorbed hydrogen structures is larger than the density of bulk liquid at critical temperature (~ 76 kg/m³). This result agrees with the experimental observation of the density of the order of 100 kg/m³ for the hydrogen adsorbed in microporous carbons, reported recently in the literature.

Keywords Adsorption · Hydrogen storage · Nanoporous carbons · Monte Carlo simulations

Introduction

During the last two decades a lot of effort has been devoted to develop a material that could store an applicable amount of hydrogen by physisorption. Computer simulations have been used to guide the experiment and to predict potential storage capacity of proposed new structures. Usually, a united atom (UA) representation of hydrogen molecule and a simplified interaction model with semi-empirical interaction parameters have been used. This approximation allowed in the past to spare the computation time. However, although the united atom model describes correctly the hydrogen adsorption at ambient temperature, it is not straightforward that this approximation is still valid at low (liquid nitrogen) temperature range. In fact, this approach totally neglects the non-spherical shape of the molecule, information that may be crucial for the precise evaluation of the packing and the structure of the adsorbed layers, and, in consequence, the amount stored. Therefore, in this paper we simulated the low temperature ($T = 77$ K) hydrogen adsorption in carbon slit-shaped nanopores using consecutively united atom (UA) and all atom (AA) representation of hydrogen molecule, and focus on the comparison of structure and density of the adsorbed hydrogen layers in both models, in the limit of high density, at gas fugacity up to 800 bar.

Interaction models

There have been a number of different approaches to model the pore system optimized to store hydrogen by physisorption [1–7], and to describe the hydrogen-hydrogen interaction

This paper belongs to Topical Collection 7th conference on Modeling & Design of Molecular Materials in Trzebnica (MDMM 2016)

Electronic supplementary material The online version of this article (doi:10.1007/s00894-016-3202-y) contains supplementary material, which is available to authorized users.

- ✉ Lucyna Firlej
Lucyna.firlej@umontpellier.fr
- ✉ Bogdan Kuchta
Bogdan.Kuchta@univ-amu.frk

¹ Group of Bioprocess and Biomedical Engineering, Wrocław University of Science and Technology, Wrocław, Poland

² Laboratoire Charles Coulomb (L2C), UMR 5221 CNRS-Université de Montpellier, Montpellier, France

³ Laboratoire MADIREL, UMR 7246 CNRS-Aix-Marseille Université, 13396 Marseille, France

⁴ Department of Physics and Astronomy, University of Missouri, Columbia, MO, USA

involved in the process. The models reported in the literature are listed in Table S1 (see Supporting information). These are semi-empirical potentials with Lennard-Jones functional form. Among them, the interaction model proposed by Silvera and Goldman [8–10] is one of the most frequently used. It was derived by fitting the solid state H₂ experimental characteristics and was successfully used to model, in particular, the hydrogen adsorption in pure carbons systems (graphite surfaces, graphene layers, and carbon nanotubes). To take into account the quadrupole-quadrupole interaction, Levesque et al. proposed a modified Lennard-Jones potential model in which the effective charges, distributed along the hydrogen molecule axis have been added: two located on both protons and one at the center between them [11]. To simulate hydrogen uptake in IRMOF-1, Yang et al. obtained the Lennard-Jones parameters of H₂-H₂ potential by fitting the experimental PVT diagrams of gaseous hydrogen [12]. The same parameters were then successfully used by Baburin et al. in GCMC calculations of hydrogen adsorption on perforated graphene [13]. Cracknell [14, 15] modeled hydrogen chemisorption in carbon nanotubes using two centers representation of rigid hydrogen molecule, with hard sphere diameter of 0.259 nm. Finally, to describe chemical reactions in hydrocarbon systems, van Duin et al. prepared the ReaxFF force field [16]. Hydrogen molecule is represented there as a single interaction site, whereas the nonbonded interactions are approximated by distance-correlated Morse potential. This approach was used to model adsorption in a variety of carbon systems: graphite [17, 18], graphene [17, 18], carbon slit pores [19–22], carbon nanotubes [19, 20], and carbon nanofoams [19, 20].

Many of the above mentioned hydrogen-hydrogen interactions models are included in the popular force field libraries: UFF [12, 23], DREIDING [24–26], cvff [26, 27], and COMPASS [28, 29]. Most of the force fields are parametrized for both: UA and AA approaches. Quantum effects are usually taken into account by adjusting force field according to Feynman-Hibbs procedure [12–15]. Some of them are explicitly implemented in modeling software (for example: MUSIC, NAMD or Materials Studio).

In the present work H₂-H₂ interaction was modeled using the Lennard-Jones (6-12) potential, with interaction parameters (defined in the Table 1): $\sigma_{\text{H}_2\text{-H}_2}$ and $\epsilon_{\text{H}_2\text{-H}_2}$ [22, 30, 31] for UA model, and $\sigma_{\text{H-H}}$ and $\epsilon_{\text{H-H}}$ [13] for the AA model. We have verified that both models give similar average energies of

H₂ adsorption on graphene: 4.5 kJ mol⁻¹ and 4.55 kJ mol⁻¹ for the UA and the AA, respectively.

To describe the H₂-wall interaction the Steele 10-4 potential already tested in [22, 32] was employed together with UA approximation. The atomic corrugation of the pore wall was neglected. The carbon-hydrogen interaction was modeled explicitly when AA hydrogen model was used ($D_0 = 0.1517$ kJ mol⁻¹ and $R_0 = 3.58217$ Å [13]).

The Feynman-Hibbs quantum correction was applied for all interactions [22, 33–35]. The interactions were cut-off beyond 12.5 Å (15 Å) in AA (UA) models, respectively.

Methods

All calculations were performed using Monte Carlo method in grand canonical ensemble (GCMC), at constant temperature $T = 77$ K, and fugacity varying from 1 to 700 bar. Two different software packages were used: Materials Studio 8.0 (MS) software (Sorptions module) for AA model of H₂ and our own code for UA approach, extensively tested and validated in the past [21, 22, 30, 31]. In grand canonical Monte Carlo simulation (μ VT ensemble) the chemical potential μ of the adsorbed phase in equilibrium with the gas reservoir is defined by gas fugacity f :

$$\mu = \mu^0 + RT \ln \left(\frac{f}{p^0} \right) \quad (1)$$

, where μ^0 – standard chemical potential, R – gas constant, T – temperature [K] and p^0 – standard pressure [kPa]. At low pressure, when the density of the gas in equilibrium with the adsorbed phase is small, the fugacity is practically identical with the gas pressure. However, when gas density increases, the difference between fugacity and the applied gas pressure is non-negligible and must be estimated. In the case of hydrogen, this difference becomes important for pressures higher than 100 bar. Therefore, for all fugacity values used in simulations we have calculated the corresponding hydrogen pressure using NIST database [36]. The simulations have been run up to 700 bar (of fugacity) which correspond to about 440 bar of the gas pressure.

The carbon pores were formed by two parallel graphene walls (slit-shaped geometry). The separation of the walls (pore width, Z), varied from $H = 0.6$ nm to $H = 3.0$ nm. For technical reasons, we used different lateral XY dimensions of the simulation box in our code (orthogonal, 4.26×4.92 nm²) and in MS software (hexagonal, 1.23×1.23 nm²). Periodic boundary conditions were applied in the XY plane in our code and in all directions in MS software.

The raw result of GCMC simulation is the total amount of the gas stored at given (f , T) conditions in the volume of the pore, (N_{tot}). The experiment measures the excess adsorption

Table 1 Parameters for Lennard-Jones potential used for united atom and all atom models

Model	Interaction	ϵ [A]	σ [K]
United atom (UA)	H ₂ – H ₂	2.958	32.4
All atom (AA)	H – H	2.59	8.84

(N_{exc}), the difference between the total amount of adsorbed gas with respect to the amount of bulk gas occupying the same volume under the same (p, T) conditions:

$$N_{exc} = N_{tot} - N_{gas} \tag{2}$$

$$N_{exc} = N_{tot} - \left(\frac{\rho_{gas} \cdot S \cdot (H - 2 \cdot R_{dead}) \cdot N_A}{M_A} \right) \tag{3}$$

,where H – pore width [\AA], $2R_{dead}$ – effective thickness of the carbon layer [\AA], S – surface of pore wall [\AA^2], N_A – Avogadro number [mol^{-1}], ρ_{NIST} – density of bulk hydrogen at given (p, T) conditions [g/ml], M_A – mass of hydrogen molecule [g mol^{-1}].

Therefore, to compare the results of numerical and adsorption experiments, the excess adsorption should be calculated from the total amount adsorbed. In small pores, this calculation is extremely sensitive to the value of the dead volume which for the nanopores is a non-negligible part of the total pore volume. We assumed that the dead volume of the pores is delimited by the distance $R_{dead} = 0.15$ nm from the centers of carbon atoms forming the pore wall. This value is close to the radius of a carbon atom ($R_C = 0.17$ nm) and was widely used in the past [31].

Results and discussion

Figure 1a shows the number of molecules adsorbed in a pore at $T = 77$ K and fugacity $f = 700$ bar, in a function of pore size. There are two plateaus on the curve corresponding to adsorption of exactly one layer between the pore walls (for pore width from 0.6 nm to 0.85 nm) and to the adsorption of exactly two layers (one layer on each pore wall) for pore width from 0.9 nm to 1.1 nm. For pores larger than 1.1 nm the number of molecules monotonically increases with no further singularities. This is a consequence of very weak H_2 - H_2

interaction which prevents any formation of multilayer structure of the adsorbed hydrogen, even at high pressure. Therefore, we have chosen to compare the structure of the adsorbed hydrogen layers simulated using either UA or AA model of hydrogen molecule for the following three representative pore widths: $H = 0.6$ nm (monolayer), 1.0 nm (one layer (contact layer) adsorbed at each pore wall), and 2.2 nm (gas adsorbed between contact layers).

Figure 1b shows the energy of adsorption as a function of the pore size, at the lowest ($f = 1$ bar) and the highest ($f = 700$ bar) simulated fugacity, calculated using all-atom interaction model. In narrow pores the hydrogen interaction with both pore walls sum up and the resulting energy of adsorption is high, independent of the value of gas pressure. As the pore size increases, the energy of adsorption becomes pressure dependent. At low pressure, the adsorption energy in largest pores ($H > 1.4$ nm) stabilizes at the value of 4.5 kJ mol^{-1} , characteristic for hydrogen adsorption on a single layer of graphene [15]. At high pressure, we initially observe a small increase of the adsorption energy (for $0.9 \text{ nm} < H < 1.1 \text{ nm}$) resulting from the contribution of H_2 - H_2 interaction to the formation of single layers (contact layers) on both pore walls. For $H > 1.1$ nm the interaction of hydrogen molecules adsorbing between the contact layers with the pore wall becomes negligible, and the adsorption progresses only because of H_2 - H_2 interaction. As a consequence, the calculated (average) energy of adsorption in the pore decreases.

Figure 2 shows the snapshots of stabilized configurations of hydrogen monolayer adsorbed in a narrow pore ($H = 0.6$ nm) at $f = 700$ bar, for all-atom (Fig. 2a) and united atom (Fig. 2b) models of hydrogen molecule. In both models the densely packed structure of the adsorbed layer is observed, although the elongated shape of H_2 molecules in the AA model compel them to adopt a slightly less dense pattern, with molecular axis mostly in the plane of the layer.

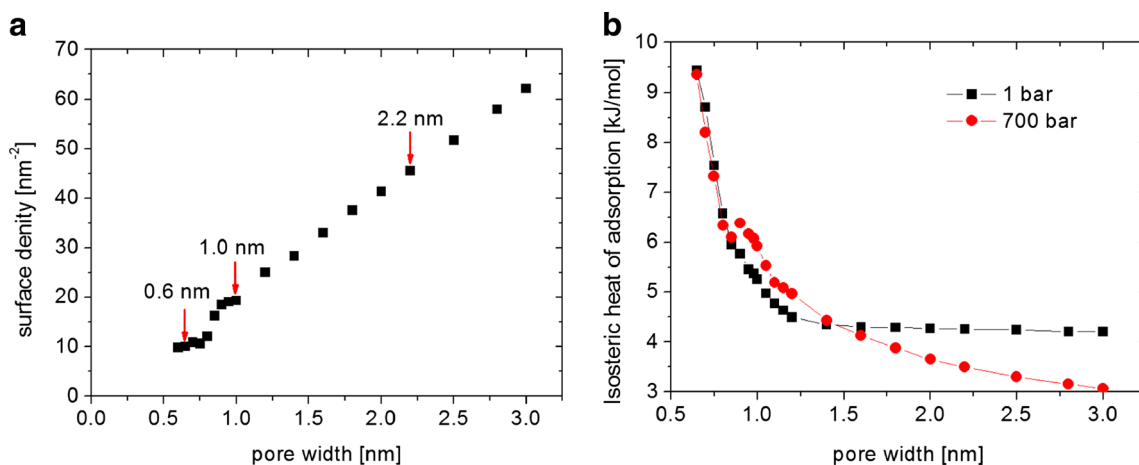


Fig. 1 a Total amount adsorbed (in number of molecules per nm^2) at $f = 700$ bar and b average energy of adsorption in a function of pore size, at $f = 1$ bar and $f = 700$ bar, in AA model

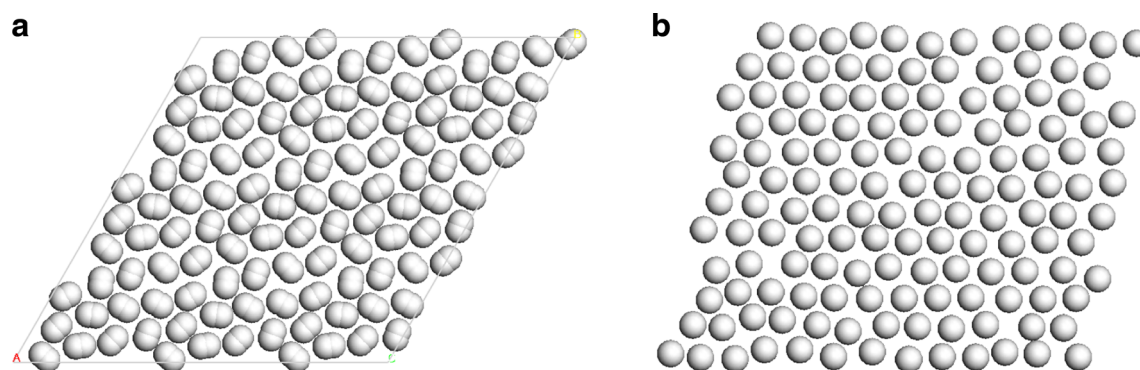


Fig. 2 Structure of hydrogen monolayer adsorbed in carbon slit pore (pore width $H = 0.6$ nm, $f = 700$ bar): **a**) all atom (AA) model, **b**) united atom (UA) model

Figure 3a, b, c compare the isotherms of hydrogen adsorption at $T = 77$ K, simulated within all-atom and united-atom approach, for the chosen pore widths. The corresponding snapshots of the adsorbed structures at $f = 700$ bar are shown in Fig. 3d, e, f. The adsorbed amount simulated using both models is similar, with the difference on the order of a few percent only. The difference is noticeable (8–10%) only in very narrow pores. In the narrowest pore studied in this work ($H = 0.6$ nm, Fig. 3a, d), when only one layer of molecules is adsorbed, the density of the layer is slightly higher for spherical representation of hydrogen molecule. In this situation, due to the elongated shape of molecules, in the AA model the geometrical constraint imposes a less dense structure of the adsorbed layer, with molecular axis parallel to the pore wall (Fig. 2a). On the contrary, when two layers are adsorbed in the pore ($H = 1.0$ nm, Fig. 3b, e) the density of the layers is higher when the AA model is applied. This fact can be again understood on a basis of geometrical considerations: in the pore which can accommodate two layers the elongated H_2 are preferentially oriented perpendicularly to the pore wall, allowing for the closer packing within the layer than in the case of superatom model of H_2 molecule and for minimization of the hydrogen–pore wall interaction. For pore width $H > 1.2$ nm, when the pore is mostly filled with not adsorbed gas, the difference between the adsorbed amounts simulated with AA and UA model vanishes (Fig. 3c, f).

Figure 4a shows the excess adsorption isotherms calculated using UA model of H_2 molecule, for pores of the width $H = 0.6$, 1.1, and 2.2 nm, as a function of gas pressure. To facilitate the comparison of the excess adsorption and total amount stored (Figs. 1a and 2a, b, c) we expressed the excess adsorption in number of molecules adsorbed per nm^2 , as this value does not depend on the wall morphology. For carbon slit-shaped pores with graphene walls the conversion factor to the usual

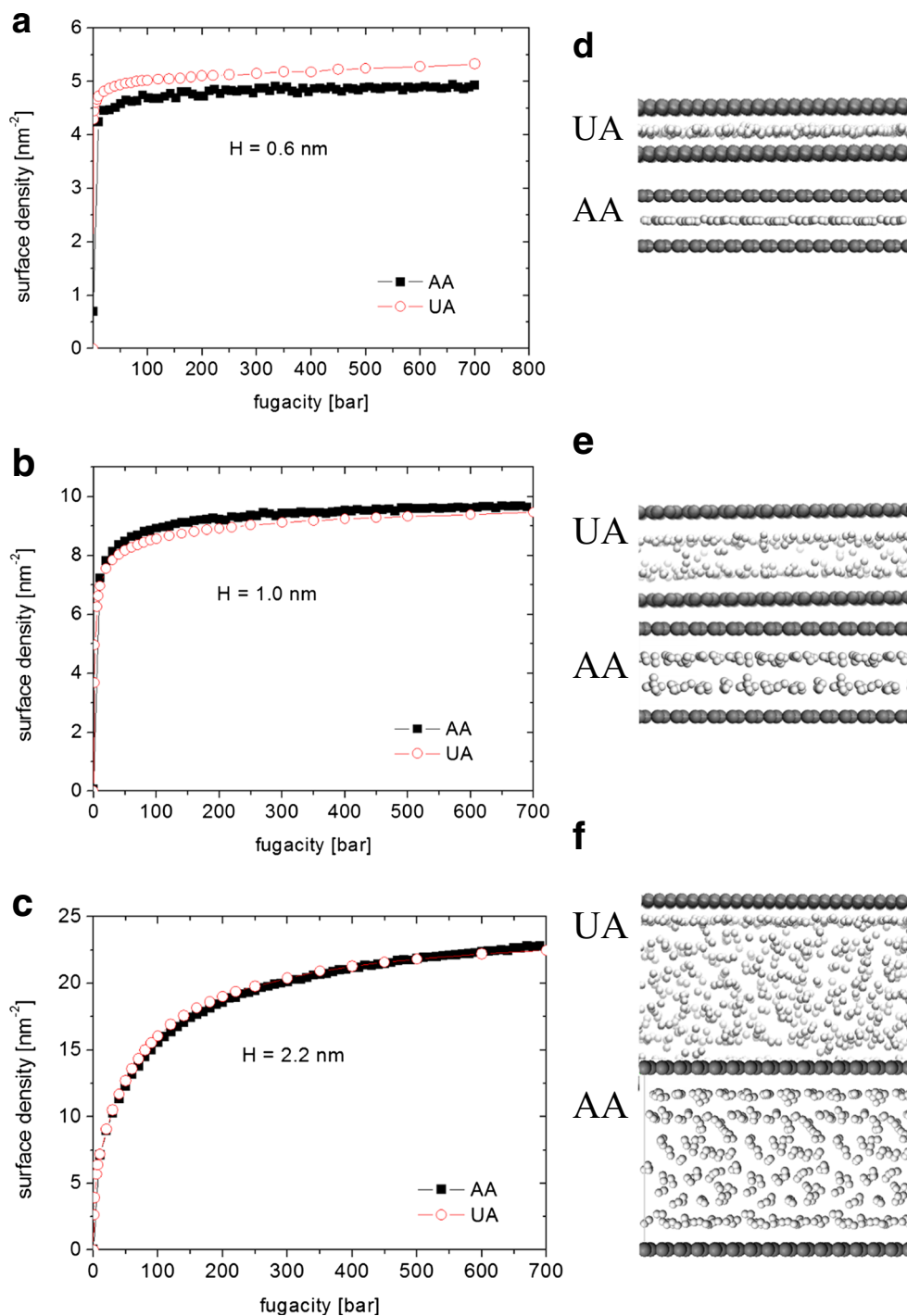
excess adsorption units (wt%) is equal to 1.14. To avoid any effects related to the shape-dependent packing, these results were validated by the calculations using the AA representation of the hydrogen molecule.

Figure 4b shows the same excess adsorption as a function of the gas density. This representation allows us to estimate directly the density of the hydrogen adsorbed in the slit pore. The experimental evaluation of the density of the fluid adsorbed in nanopores, especially at high pressures, is challenging, and only a few such studies are reported in the literature. Recently, the density of hydrogen confined in microporous activated carbon TE7 was measured by Ting et al. [37]. At 77 K and at the gas pressure of 170 bar, estimated density of the adsorbed hydrogen was $101 \pm 2 \text{ kg m}^{-3}$. This value is significantly larger than the density of bulk fluid at the same (p, T) conditions ($\sim 45 \text{ kg m}^{-3}$, [36]), and larger than the density of liquid hydrogen at critical temperature ($T = 33$ K) at this pressure ($\sim 76 \text{ kg m}^{-3}$, [36]). For the pores larger than 1.0 nm, when at least one layer of hydrogen molecules is adsorbed at each pore wall, the density of the adsorbed layer calculated from our simulations is larger than 95 kg m^{-3} . This value is estimated from the linear dependence of the excess adsorption at high pressure (density, Fig. 4b) using the general formula (2):

$$N_{\text{exc}} = N_{\text{tot}} - \rho_{\text{gas}} V_a = \rho_{\text{film}} V_a - \rho_{\text{gas}} V_a = (\rho_{\text{film}} - \rho_{\text{gas}}) V_a \quad (4)$$

where V_a is the adsorbed hydrogen volume and ρ_{film} is the layer density. Assuming that the film density ρ_{film} is constant after it attains the maximum capacity at the pressure corresponding to the maximal excess adsorption, the linear excess adsorption (Fig. 4b) at high density depends only on the gas density ρ_{gas} . Therefore, one can estimate the maximal film density from the extrapolation of the linear dependence $N_{\text{exc}}(\rho_{\text{gas}})$: for $N_{\text{exc}} = 0$, $\rho_{\text{film}} = \rho_{\text{gas}} \approx 95 \text{ kg m}^{-3}$. This result is in good

Fig. 3 Simulated hydrogen adsorption isotherms at $T = 77$ K (*left panel*) and instantaneous configurations of molecules adsorbed at $f = 700$ bar in carbon slit pores (*right panel*). Both: AA and UA results are shown, for three pore sizes: 0.6 nm (**a** and **d**), 1.0 nm (**b** and **e**), 2.2 nm (**c** and **f**)



agreement with the experimental result of Ting et al. [37] and confirms that adsorbed fluids form very dense layers inside the pores of nanometric size. It is due to the cumulative effect of interaction of gas molecules with both pore walls. In the ultramicropores ($H < 1$ nm), when only one layer of gas can be adsorbed between pore walls, the density of the layer is even larger (see Fig. 4b, $H = 0.6$ nm).

Conclusions

In this paper we reported the simulated low temperature hydrogen adsorption in carbon slit-shaped nanopores, for the wide range of pore widths (from 0.6 nm to 2.5 nm) and gas pressures (up to 400 bar). We showed that the use of either united atom (UA) or all atom (AA) representations of hydrogen molecule leads to the quantitatively similar results, even at low

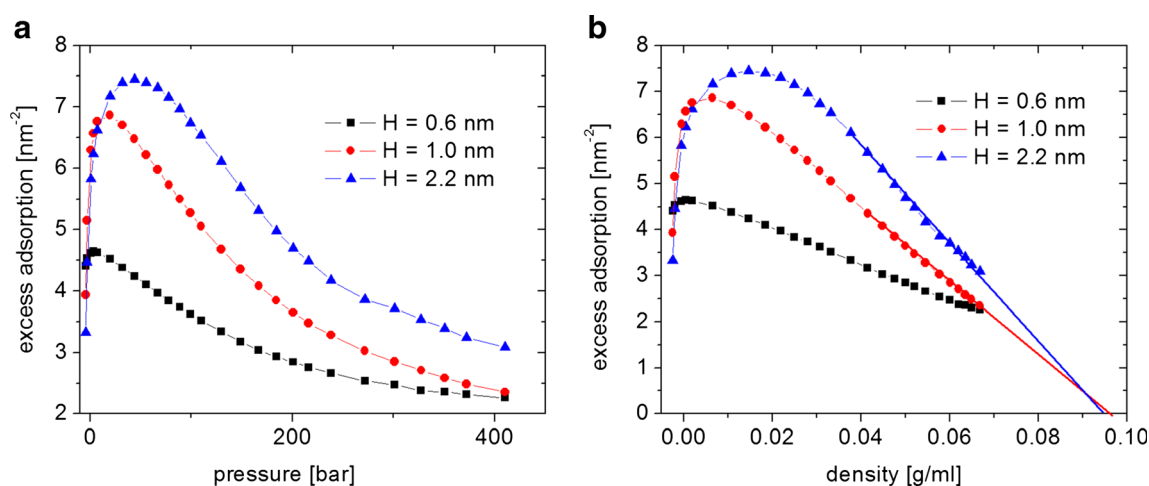


Fig. 4 Excess adsorption a function of **a**) pressure, **b**) bulk gas density for three pores containing respectively one (*squares*), two (*circles*), and more (*triangles*) layers adsorbed inside the pore

temperature (77 K) and in the limit of high gas pressure. Small differences (less than 10% of the amount stored) are observed only for the narrower pores ($H < 1$ nm), when the slit geometry forces the hydrogen molecules represented as diatoms to adopt a parallel to the pore wall arrangement. Such narrow carbon pores are usually not prepared experimentally.

We also showed that at highest applied pressures (of the order of 400 bar, corresponding to the fugacity used in computer simulations of nearly 700 bar), the density of the adsorbed hydrogen layer is high, larger than the density of bulk liquid hydrogen at critical temperature. This effect is due to the increase of the effective isosteric heat of adsorption in very narrow pores: for $H < 1$ nm the effective energy of hydrogen interaction with the pore wall practically doubles. Such extreme conditions (narrow pores, low temperature, high pressure) are hardly realized experimentally. However, the recent experimental studies performed on microporous TE7 carbons [37] ($H \sim 1.1$ nm) at $T = 77$ K and $P = 170$ bar showed that the density of the adsorbed layer overpasses 100 kg/m^3 . Our estimations at the same temperature and at $P = 400$ bar, for both UA and AA model of hydrogen molecule are of the same order of magnitude and confirm that the adsorbed hydrogen structure is densely packed at these conditions.

Acknowledgements Support from French National Research Agency (ANR) grant No. ANR-14-CE05-0009 HYSTOR is acknowledged. JR is partially supported by the Polish National Science Center (NCN, grant no. 2015/17/B/ST8/00099). The calculations have been partially performed at the WCSS computer center of The Wrocław University of Science and Technology, grant no 33.

References

- Patchkovskii S, Tse JS, Yurchenko SN et al (2005) Graphene nanostructures as tunable storage media for molecular hydrogen. *Proc Natl Acad Sci U S A* 102:10439–10444. doi:10.1073/pnas.0501030102
- Cabria I, López MJ, Alonso JA (2007) The optimum average nanopore size for hydrogen storage in carbon nanoporous materials. *Carbon N Y* 45:2649–2658. doi:10.1016/j.carbon.2007.08.003
- Alfonso Alonso J, Cabria I, Jose Lopez M (2013) Simulation of hydrogen storage in porous carbons. *J Mater Res* 28:589–604. doi:10.1557/jmr.2012.370
- Peng L, Morris JR (2010) Prediction of hydrogen adsorption properties in expanded graphite model and in nanoporous carbon. *J Phys Chem C* 114:15522–15529. doi:10.1021/jp104595m
- Martínez-Mesa A, Yurchenko SN, Patchkovskii S et al. (2011) Influence of quantum effects on the physisorption of molecular hydrogen in model carbon foams. *J Chem Phys* 135:214701. doi:10.1063/1.3664621
- Jagiello J, Betz W (2008) Characterization of pore structure of carbon molecular sieves using DFT analysis of Ar and H₂ adsorption data. *Microporous Mesoporous Mater* 108:117–122. doi:10.1016/j.micromeso.2007.03.035
- Peng LJ, Morris JR (2012) Structure and hydrogen adsorption properties of low density nanoporous carbons from simulations. *Carbon N Y* 50:1394–1406. doi:10.1016/j.carbon.2011.11.012
- Arellano JS, Molina LM, Rubio A, Alonso JA (2000) Density functional study of adsorption of molecular hydrogen on graphene layers. *J Chem Phys* 112:11. doi:10.1063/1.481411
- Silvera IF, Goldman VV (1978) The isotropic intermolecular potential for H₂ and D₂ in the solid and gas phases. *J Chem Phys* 69:4209–4213. doi:10.1063/1.437103
- Wang Q, Johnson JK (1999) Molecular simulation of hydrogen adsorption in single-walled carbon nanotubes and idealized carbon slit pores. *J Chem Phys* 110:577–586. doi:10.1063/1.478114
- Levesque D, Gicquel A, Darkrim FL, Kayiran SB (2002) Monte Carlo simulations of hydrogen storage in carbon nanotubes. *J Phys Condens Matter* 14:9285–9293
- Yang Q, Zhong C (2005) Molecular simulation of adsorption and diffusion of hydrogen in metal-organic frameworks. *J Phys Chem B*. doi:10.1021/jp051903n
- Baburin IA, Klechikov A, Mercier G et al. (2015) Hydrogen adsorption by perforated graphene. *Int J Hydrog Energy* 40:6594–6599. doi:10.1016/j.ijhydene.2015.03.139
- Cracknell RF (2001) Computer simulation of hydrogen adsorption on graphitic materials. *Mol Simul* 27:287–293. doi:10.1080/08927020108031354
- Cracknell RF (2002) Simulation of hydrogen adsorption in carbon nanotubes. *Mol Phys* 100:2079–2086. doi:10.1080/00268970210130236

16. Van Duin ACT, Dasgupta S, Lorant F, Goddard WA (2001) ReaxFF: a reactive force field for hydrocarbons. *J Phys Chem A* 105:9396–9409. doi:10.1021/jp004368u
17. Simon J-M, Haas O-E, Kjelstrup S (2010) Adsorption and desorption of H₂ on graphite by molecular dynamics simulations. *J Phys Chem C* 114:10212–10220. doi:10.1021/jp1011022
18. Wu C-D, Fang T-H, Lo J-Y, Feng Y-L (2013) Molecular dynamics simulations of hydrogen storage capacity of few-layer graphene. *J Mol Model* 19:3813–3819. doi:10.1007/s00894-013-1918-5
19. Kumar K, Salih A, Lu L et al. (2011) Molecular simulation of hydrogen physisorption and chemisorption in nanoporous carbon structures. *Adsorpt Sci Technol* 29:799–818. doi:10.1260/0263-6174.29.8.799
20. Buch V (1994) Path integral simulations of mixed para-D₂ and ortho-D₂ clusters: the orientational effects. *J Chem Phys* 100:7610. doi:10.1063/1.466854
21. Roszak R, Firlej L, Roszak S et al. (2015) Hydrogen storage by adsorption in porous materials: is it possible? *Colloids Surf A Physicochem Eng Asp* 496:69–76. doi:10.1016/j.colsurfa.2015.10.046
22. Kuchta B, Firlej L, Pfeifer P, Wexler C (2010) Numerical estimation of hydrogen storage limits in carbon-based nanospaces. *Carbon N Y* 48:223–231. doi:10.1016/j.carbon.2009.09.009
23. Rappe AK, Casewit CJ, Colwell KS et al. (1992) UFF, a full periodic table force field for molecular mechanics and molecular dynamics simulations. *J Am Chem Soc* 114:10024–10035. doi:10.1021/ja00051a040
24. Mayo SL, Olafson BD, Goddard WA (1990) DREIDING: a generic force field for molecular simulations. *J Phys Chem* 94:8897–8909. doi:10.1021/j100389a010
25. Assfour B, Seifert G (2009) Hydrogen storage in 1D nanotube-like channels metal-organic frameworks: effects of free volume and heat of adsorption on hydrogen uptake. *Int J Hydrog Energy* 34:8135–8143. doi:10.1016/j.ijhydene.2009.08.009
26. Künzel D, Markert T, Gross A, Benoit DM (2009) Bis(terpyridine)-based surface template structures on graphite: a force field and DFT study. *Phys Chem Chem Phys* 11:8867–8878. doi:10.1039/b907443k
27. Consistent Valence Forcefield (CVFF). <http://www.quimica.urv.es/~bo/MOLMOD/General/Forcefields/CVFF.html>
28. Yang J, Ren Y, Tian A, Sun H (2000) COMPASS force field for 14 inorganic molecules, He, Ne, Ar, Kr, Xe, H₂, O₂, N₂, NO, CO, CO₂, NO₂, CS₂, and SO₂, in liquid phases. *J Phys Chem B* 104:4951–4957. doi:10.1021/jp992913p
29. Sun H (1998) COMPASS: an ab initio force-field optimized for condensed-phase applications overview with details on alkane and benzene compounds. *J Phys Chem B* 102:7338–7364. doi:10.1021/jp980939v
30. Kuchta B, Firlej L, Roszak S et al. (2010) Influence of structural heterogeneity of nanoporous sorbent walls on hydrogen storage. *Appl Surf Sci* 256:5270–5274. doi:10.1016/j.apsusc.2009.12.116
31. Firlej L, Pfeifer P, Kuchta B (2013) Understanding universal adsorption limits for hydrogen storage in nano porous systems. *Adv Mater* 25:5971–5974. doi:10.1002/adma.201303023
32. Siderius DW, Gelb LD (2011) Extension of the Steele 10-4-3 potential for adsorption calculations in cylindrical, spherical, and other pore geometries. *J Chem Phys* 135:84703. doi:10.1063/1.3626804
33. Kovalev VL, Yakunchikov AN (2009) Simulation of hydrogen adsorption in carbon nanotubes. *Fluid Dyn Mekhanika Zhidkosti i Gaza* 44:15–4628. doi:10.1134/S0015462809030168
34. Firlej L, Rogacka J, Walczak K, Kuchta B (2016) Hydrogen adsorption on surfaces with different binding energy. *Chem Data Collect*. doi:10.1016/j.cdc.2016.02.002
35. Kowalczyk P, Tanaka H, Hołyst R et al. (2005) Storage of hydrogen at 303 K in graphite slitlike pores from grand canonical Monte Carlo simulation. *J Phys Chem B* 109:17174–17183. doi:10.1021/jp0529063
36. NIST Chemistry WebBook. <http://webbook.nist.gov/chemistry/>
37. Ting VP, Ramirez-Cuesta AJ, Bimbo N et al. (2015) Direct evidence for solid-like hydrogen in a nanoporous carbon hydrogen storage material at supercritical temperatures. *ACS Nano* 9:8249–8254. doi:10.1021/acsnano.5b02623